AFRL-RV-PS-
TR-2016-0136

GROUND TRUTH EVENTS WITH SOURCE GEOMETRY IN EURASIA AND THE MIDDLE EAST

Sharmin Shamsalsadati, et al.

Department of Geosciences
Penn State University
University Park, PA 16802

02 June 2016

Final Report

AIR FORCE RESEARCH LABORATORY
Space Vehicles Directorate
3550 Aberdeen Ave SE
AIR FORCE MATERIEL COMMAND
KIRTLAND AIR FORCE BASE, NM 87117-5776

DTIC COPY

NOTICE AND SIGNATURE PAGE

Using Government drawings, specifications, or other data included in this document for any purpose other than Government procurement does not in any way obligate the U.S. Government. The fact that the Government formulated or supplied the drawings, specifications, or other data does not license the holder or any other person or corporation; or convey any rights or permission to manufacture, use, or sell any patented invention that may relate to them.

This report was cleared for public release by the PRS OPSEC Office and is available to the general public, including foreign nationals. Copies may be obtained from the Defense Technical Information Center (DTIC) (http://www.dtic.mil).

AFRL-RV-PS-TR-2016-0136 HAS BEEN REVIEWED AND IS APPROVED FOR PUBLICATION IN ACCORDANCE WITH ASSIGNED DISTRIBUTION STATEMENT.

//SIGNED//	//SIGNED//
Dr. Frederick Schult Program Manager, AFRL/RVBYE	Dr. Thomas R. Caudill, Acting Chief AFRL Battlespace Environment Division

This report is published in the interest of scientific and technical information exchange, and its publication does not constitute the Government's approval or disapproval of its ideas or findings.

REPORT DOCUMENTATION PAGE

Form Approved
OMB No. 0704-0188

1. REPORT DATE *(DD-MM-YYYY)*	**2. REPORT TYPE**	**3. DATES COVERED** *(From - To)*
02-06-2016	Final Report	24 Apr 2014 – 30 Apr 2016

4. TITLE AND SUBTITLE
Ground Truth Events with Source Geometry in Eurasia and the Middle East

5a. CONTRACT NUMBER
FA9453-14-C-0213

5b. GRANT NUMBER

5c. PROGRAM ELEMENT NUMBER
62601F

6. AUTHOR(S)
Sharmin Shamsalsadati, Andrew A. Nyblade, John Paul O'Donnell, and Richard Brazier

5d. PROJECT NUMBER
1010

5e. TASK NUMBER
PPM00020373

5f. WORK UNIT NUMBER
EF127046

7. PERFORMING ORGANIZATION NAME(S) AND ADDRESS(ES)
Department of Geosciences
Penn State University
University Park, PA 16802

8. PERFORMING ORGANIZATION REPORT NUMBER

9. SPONSORING / MONITORING AGENCY NAME(S) AND ADDRESS(ES)
Air Force Research Laboratory
Space Vehicles Directorate
3550 Aberdeen Avenue SE
Kirtland AFB, NM 87117-5776

10. SPONSOR/MONITOR'S ACRONYM(S)
AFRL/RVBYE

11. SPONSOR/MONITOR'S REPORT NUMBER(S)
AFRL-RV-PS-TR-2016-0136

12. DISTRIBUTION / AVAILABILITY STATEMENT
Approved for public release; distribution is unlimited. (OPS-16-12237 dtd 18 Jul 2016)

13. SUPPLEMENTARY NOTES

14. ABSTRACT
In this project, Ground Truth (GT) 5 level seismic events in the Middle East and East Africa have been identified and a range of source properties for these events have been determined. The empirically based GT criteria developed by Boomer et al. (2010, 2013) has been used to identify 15 new GT5 events in Saudi Arabia, 5 in Ethiopia, and 10 in Tanzania with magnitudes of 3 or greater. Source parameters were obtained through moment tensor inversions for a number of the events where available waveforms were of sufficient quality. In addition, other source properties, such as seismic moment, stress drop, and corner frequency were also obtained for these events using the Andrews (1986) method. In total, given the quality of available data, we were able to obtain source parameters and other source properties for 8 events in Saudi Arabia, 3 in Tanzania, and 3 in Ethiopia.

15. SUBJECT TERMS
seismic location; seismic ground truth; seismic moment tensor

16. SECURITY CLASSIFICATION OF:			**17. LIMITATION OF ABSTRACT**	**18. NUMBER OF PAGES**	**19a. NAME OF RESPONSIBLE PERSON**
a. REPORT	**b. ABSTRACT**	**c. THIS PAGE**			Dr. Frederick Schult
Unclassified	Unclassified	Unclassified	Unlimited	36	**19b. TELEPHONE NUMBER** *(include area code)*

This page is intentionally left blank.

Table of Contents

List of Figures

List of Tables

This page is intentionally left blank.

1. SUMMARY

In this project, Ground Truth (GT) 5 level seismic events in the Middle East and East Africa have been identified and a range of source properties for these events have been determined. The empirically based GT criteria developed by Boomer et al. (2010, 2013) has been used to identify 15 new GT5 events in Saudi Arabia, 5 in Ethiopia, and 10 in Tanzania with magnitudes of 3 or greater. Source parameters were obtained through moment tensor inversions for a number of the events where available waveforms were of sufficient quality. In addition, other source properties, such as seismic moment, stress drop, and corner frequency were also obtained for these events using the Andrews (1986) method. In total, given the quality of available data, we were able to obtain source parameters and other source properties for 8 events in Saudi Arabia, 3 in Tanzania, and 3 in Ethiopia.

2. INTRODUCTION

Calibration events at a Ground Truth (GT) 5 level or better with source geometry for several seismic events in Saudi Arabia, Tanzania, and Ethiopia have been obtained. The empirically based GT criteria developed by Boomer et al. (2010, 2013) has been used to identify the GT events and moment tensor inversion software developed by Herrmann (2013) has been used to estimate moment tensor elements, moment magnitudes, focal mechanisms, and source depths. For each region, crustal and upper mantle seismic velocity models were used in the source modeling derived from published studies using both active and passive source seismic data. Other source properties, including seismic moment, corner frequency, radiated energy, and stress drop have been obtained using spectra for *S* waves following the method of Andrews (1986).

3. TECHNICAL APPROACH

3.1. GROUND TRUTH

Boomer et al. (2010) tested the existing global GT criteria against reference GT mine events recorded on a sparse regional network in southern Africa and demonstrated that the global GT criteria from Bondar et al. (2004) and Bondar and McLaughlin (2009) presently employed by the community can be overly restrictive for certain tectonic settings. This motivated them to develop empirically based GT5$_{95\%}$ criteria specific to the Kaapvaal Craton in southern Africa. They showed that many events recorded on the southern African seismic network (Carlson et al., 1996), while satisfying the regionally tailored criteria, did not qualify as GT5$_{95\%}$ events according to the more stringent constraints of the global criteria. This highlighted the fact that events in strategically important locations, which fail to qualify as GT5 according to the existing global criteria, could potentially be re-classified provided that regionally tailored criteria were available.

Boomer et al. (2013) subsequently developed empirically based ground-truth (EBGT) criteria for the Main Ethiopian Rift and the Tibetan Plateau, regions of contrasting and

considerable geological complexity compared to the Kaapvaal Craton. The criteria were used to identify 34 new GT5$_{95\%}$ events with magnitudes greater than 2.1 in Ethiopia and 27 new GT5$_{95\%}$ events with magnitudes greater than 2.5 in Tibet. Taken together, the results indicate that as geological complexity increases, progressively more restrictive network geometries are necessary in order to locate seismic events to a given degree of accuracy.

Unfortunately, the GT data necessary to formally develop tailored EBGT for regions of interest are often lacking, in particular for the events used in this study for Saudi Arabia and Tanzania. In response, we have invoked the principal of criteria transfer between tectonic analogues and applied the Kaapvaal Craton criteria to the Precambrian Shield of western Saudi Arabia and to the Tanzania Craton and adjacent Mozabmique Belt in Tanzania to identify GT5 events in these regions. The EBGT criteria for the Main Ethiopian Rift developed by Boomer et al. (2013) have been used for the Ethiopia events included in this study.

The GT locations and origin times provided have been obtained using the HYPOSELLIPSE location code and local, well constrained crustal velocity models obtained from published studies (see references below in section 4.0) and carefully hand picked arrival times.

3.2. SOURCE MECHANISMS

Source mechanisms and other source parameters for a number of the GT5 events found in Saudi Arabia, Tanzania, and Ethiopia have been obtained. Grid search and moment tensor inversion methods have been used to obtain moment tensor elements, source depth, moment magnitude, and seismic moment. The codes described in Herrmann (2013) have been used for both the grid search and moment tensor inversion. The grid search code solves for a double couple source and the moment tensor code solves for a deviatoric source. The deviatoric source model is designated by five independent moment tensor elements, whereas the full moment tensor inversion solves for 6 independent moment tensor elements. The latter method is less stable and sometimes results in trade-offs between the source components and other source parameters, such as depth. Therefore, full moment tensor inversion does not necessarily provide a better source model in comparison to the deviatoric moment tensor inversion (e.g. Belachew et al., 2013). Consequently, using the available three-component high quality data, we only inverted for deviatoric moment tensors. Prior to using the data for modeling the sources, the instrument responses were deconvolved from the data, and the waveforms were low frequency bandpass filtered to include mainly the surface waves. Local 1D velocity models were used to calculate the Green's functions used in the source modeling.

The success of the modeling process can be assessed using the goodness of fit between the observed and predicted seismograms. For the grid search, the goodness of fit parameter used is the reduction of weighted variance, which results in values in the range of [0, 1]. The depth that yields the largest variance reduction (best fit) is chosen as the centroid depth. The grid search was performed over a large range in focal depth. For each source depth, the grid search method determines the best fitting source defined by the strike, dip, and rake angles. The source depth with the largest variance reduction was selected as the best solution.

Similarly, the inversion for a deviatoric moment tensor solution was performed over the same large range in focal depth. In this method, a least-squares minimization of misfit between recorded and synthetic seismograms was used to assess the goodness of fit. Several sets of inversions were performed using various frequency bands, number of stations, and source methods to ensure stability of the inversions.

3.3. OTHER SOURCE PARAMETERS

Other source parameters, including radiated energy, corner frequency, seismic moment, and static stress drop were calculated using a spectral technique (Richardson & Jordan, 2002; Andrews, 1986). The process entails separating event and station spectra and median-stacking each event's spectra along with integrating the results up to the Nyquist frequency to determine S_D, the integral of the displacement power spectra (see Equation 6 of Andrews, 1986), S_V, the integral of the velocity power spectra (see Equation 7 of Andrews, 1986), and A^2, the acceleration power spectral level (see Equation 19 of Andrews, 1986). These are used to determine the radiated energy (E), seismic moment (M_0), and static stress drop ($\Delta\sigma$) as follows:

$$E = 4\pi\rho v S_V \tag{1}$$

$$M_0 = \frac{8\pi\rho v^3 S_D^{(3/4)}}{\Re S_V^{(1/4)}} \tag{2}$$

$$\Delta\sigma = \frac{2\pi f_0 \rho A^2}{C\Re} \tag{3}$$

with the corner frequency given by

$$f_0 = \left(\sqrt{S_V / S_D}\right) / 2\pi. \tag{4}$$

In these equations, ρ is the rock density, ν is wavespeed, $\Re$ is a constant based radiation pattern, which is $\sqrt{4/15}$ for *P*-waves and $\sqrt{2/15}$ for *S*-waves (Richardson, 2002). *C* is also a small constant, chosen as 2.01 for *P*-waves and 1.32 for *S*-waves (Madariaga, 1976). An advantage of this method is that the exponent of the spectral rolloff is not a fixed parameter, as in the case of fitting spectra with a Brune-type curve.

4. RESULTS AND DISCUSSION

4.1. LUNAYYIR, WESTERN SAUDI ARABIA GT RESULTS

In April 2009, a swarm of earthquakes began on the eastern side of the Cenozoic Lunayyir Harrat in west-central Saudi Arabia, with a magnitude > 5 main shock occurring on May 19. In response to the onset of activity, a network of 29 seismometers was installed jointly by the Saudi Geological Survey (SGS), King Abdulaziz City for Science and Technology (KACST) and King Saud University (KSU), recording thousands of events through June 2009.

Although the Lunayyir Harrat is a Cenozoic volcanic field, it sits on a Precambrian Shield and the crustal structure is well known (e.g., Hansen et al., 2013; Juliá et al., 2003; Kumar et al., 2002, Mooney et al., 1985). As such, to identify candidate GT5 events from the Lunayyir

swarm we applied the EBGT criteria developed by Boomer et al. (2010) for the tectonically analogous Kaapvaal Craton. Although the broadband SGS data was unavailable, waveform data from the 16 KACST and KSU short period stations sampling at 100 sps were made available to the PI by Dr. Abdullah Al-Amri.

Fifteen events of magnitude greater than 3.5 were identified as meeting the EBGT Kaapvaal Craton criteria and relocated using handpicked Pg arrival times in conjunction with a crustal velocity model from Hansen et al. (2013). Event information is given in Table 1 and event and station locations are shown in Figure 1, together with focal mechanisms obtained for 8 of the events. Magnitudes shown are local magnitude determinations.

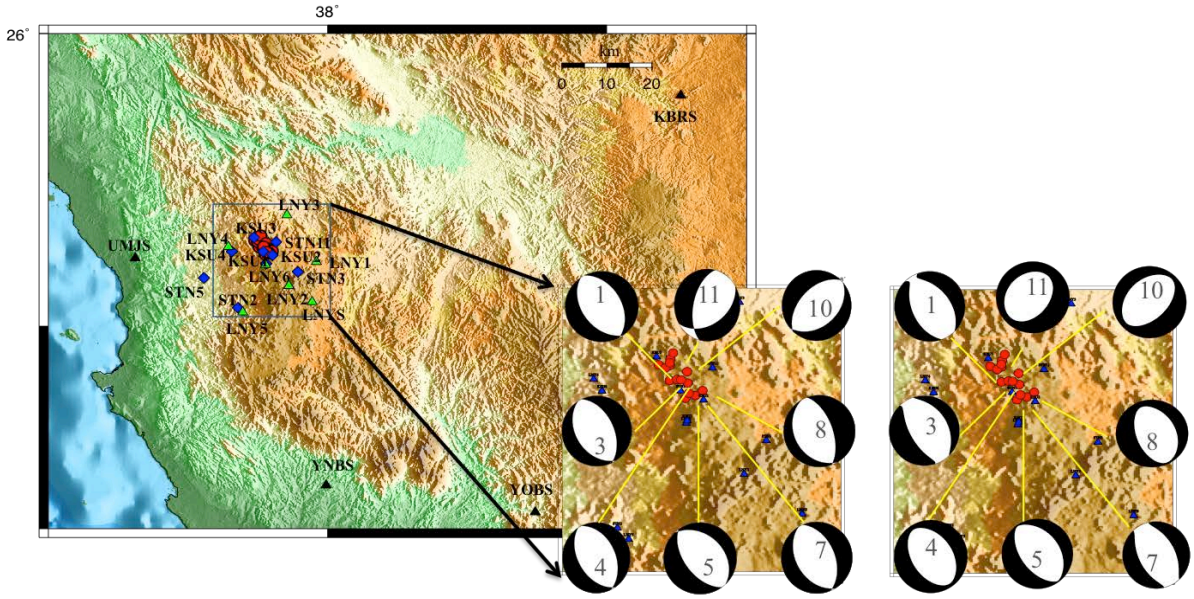

Figure 1. Map showing events, stations, and mechanisms for Saudi Arabia. Topographic map showing GT event locations (red circles) from Table 1 and seismic stations. *Short-period stations from the King Saud University network are shown with blue diamonds, and broadband stations operated by the Saudi Arabian Geological Survey networks are shown with black and green triangles. Inset shows fault plane solutions using (left) a grid search method and (right) a deviatoric moment tensor inversion for events listed in Table 3.*

Table 1. Event locations and origin times for GT5 events in Saudi Arabia.

Event #	Year	Month	Day	Hour	Minute	Second	Latitude	Longitude	M_L
1	2009	5	18	23	43	36	25.292	37.7383	3.5
2	2009	5	19	15	50	45	25.2698	37.7542	3.5
3	2009	5	19	16	54	29	25.2712	37.7647	5.1
4	2009	5	19	17	13	26	25.291	37.7544	4.2
5	2009	5	19	17	34	59	25.2876	37.7483	5.4
6	2009	5	19	19	21	28	25.3001	37.755	4
7	2009	5	19	19	33	22	25.2948	37.7543	4
8	2009	5	19	19	44	19	25.3087	37.7591	3.6
9	2009	5	20	21	35	19	25.2447	37.7766	3.9
10	2009	5	21	22	3	16	25.2821	37.779	3.6
11	2009	5	30	8	31	58	25.2663	37.7801	3.6
12	2009	6	20	12	59	13	25.2709	37.7705	3.7
13	2009	6	22	11	2	43	25.2556	37.8014	3.8
14	2009	7	3	3	54	0	25.2487	37.791	3.7
15	2009	7	4	6	32	24	25.2517	37.7816	3.8

4.2. LUNAYYIR, WESTERN SAUDI ARABIA SOURCE PARAMETERS

Of the 15 earthquakes analyzed, we could obtain source parameters using the grid search and moment tensor inversion methods for 8 of them (Table 2). The data for the other events was of insufficient quality to obtain stable modeling results. An average velocity model for typical Precambrian crust (Table 3) was used (Herrmann, personal communication). Figure 2 shows the comparison between synthetic and observed waveforms for the optimum depths for each event. This figure also illustrates how the mechanisms and goodness of the fit vary with depth for these events.

In Table 2, comparison of the goodness of the fit between the observed and calculated waveforms was performed using a grid search (DC), and Deviatoric Moment Tensor Inversion (DVMT). Percentages of CLVD and DC components estimated using these methods are listed in the last two columns. GCMT solutions are marked in red for comparison. Depth, magnitude, strike, dip and rake from the deviatoric inversions are also listed.

Table 2. Source parameters for Saudi Arabian Events

Event #	Depth [km]	M_W	Goodness of the fit (%) DC	DVMT	Strike (Deg)	Dip (Deg)	Rake (Deg)	%CLVD, %DC
1	2	3.5	61	75	139/338	44/48	-104/-77	2 , 98
3	3	5	84	90	146/331	33/57	-94/-87	11 , 89
		5			145/329	42/48	-94/-87	
4	3	4.4	87	93	145/328	42/48	-92/-88	10 , 90
5	2	5.7	93	96	144/323	37/53	-90/-90	3 , 97
		5.7			143/320	42/48	-88/-92	
7	3	3.7	85	93	151/333	43/47	-91/-89	14 , 86
8	3	3.4	74	90	149/341	37/54	-100/-83	9 , 91
10	3	3.9	96	98	43/227	38/53	-93/-88	14 , 86
11	2	3.5	71	88	47/217	34/56	-82/-95	34 , 66

Table 3. 1D velocity model used to calculate Green's functions for Saudi Arabian events.

Thickness (km)	*P*-wave velocity (km/s)	*S*-wave velocity (km/s)	Density (kg/m^3)
1	5.0000	2.8900	2500
9	6.1000	3.5200	2730
10	6.4000	3.7000	2820
20	6.7000	3.8700	2902
∞	8.1500	4.7000	3364

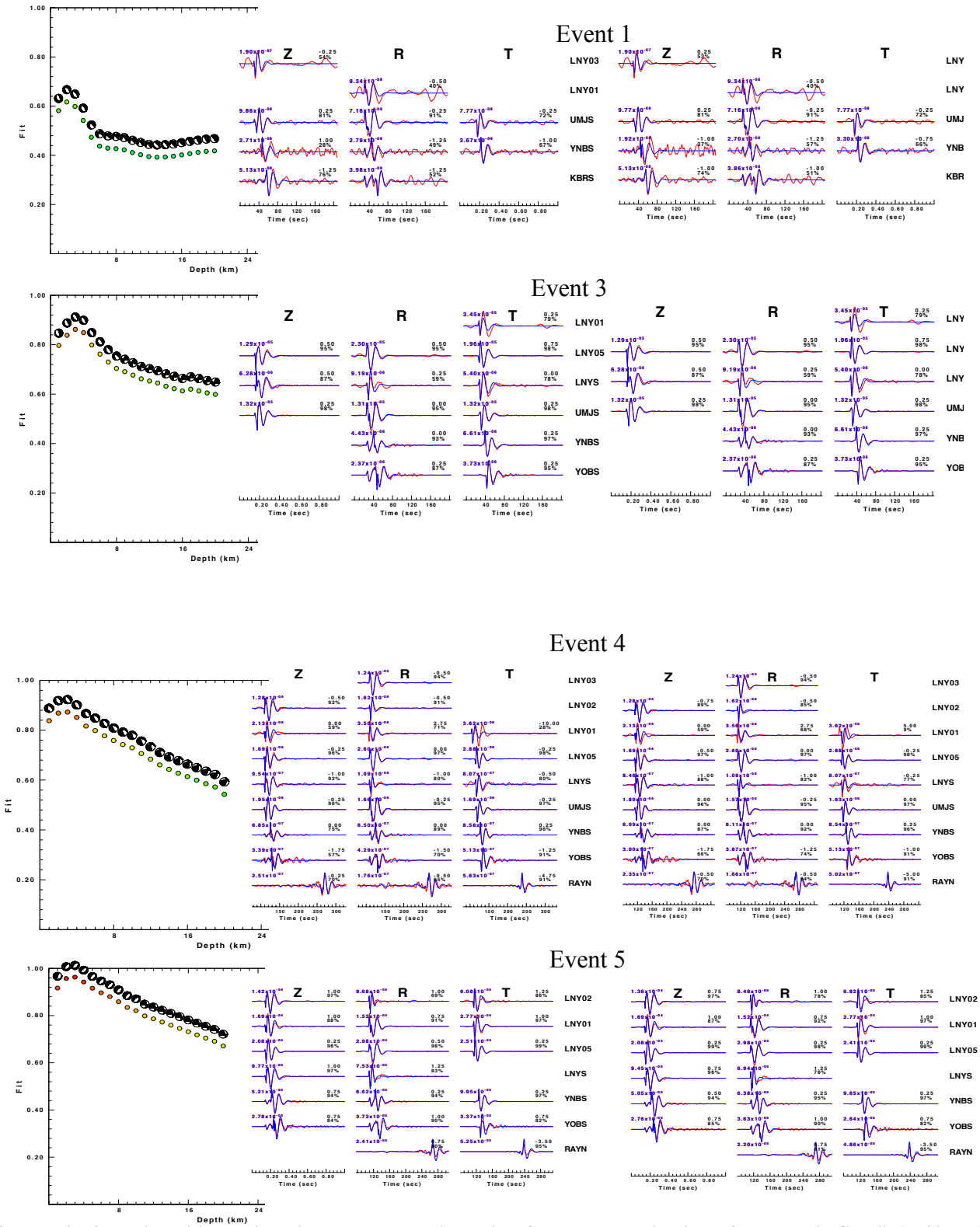

Figure 2. Results from the grid search and moment tensor inversion for source mechanisms for events in Saudi Arabia. *The event numbers are the same as in Table 2. The panel on the left for each event shows the depth sensitivity of the goodness of fit parameter for the grid search. The panel of data in the middle shows the waveform fits for the grid search and the panel of data on the right is for the moment tensor inversion. The observed waveforms are in red and the matching synthetics are in blue for the best fitting solutions. The number on the top of the waveforms gives the time shift between the observed and synthetic waveforms. The focal mechanisms for the best fitting solutions are shown for each event in Figure 1.*

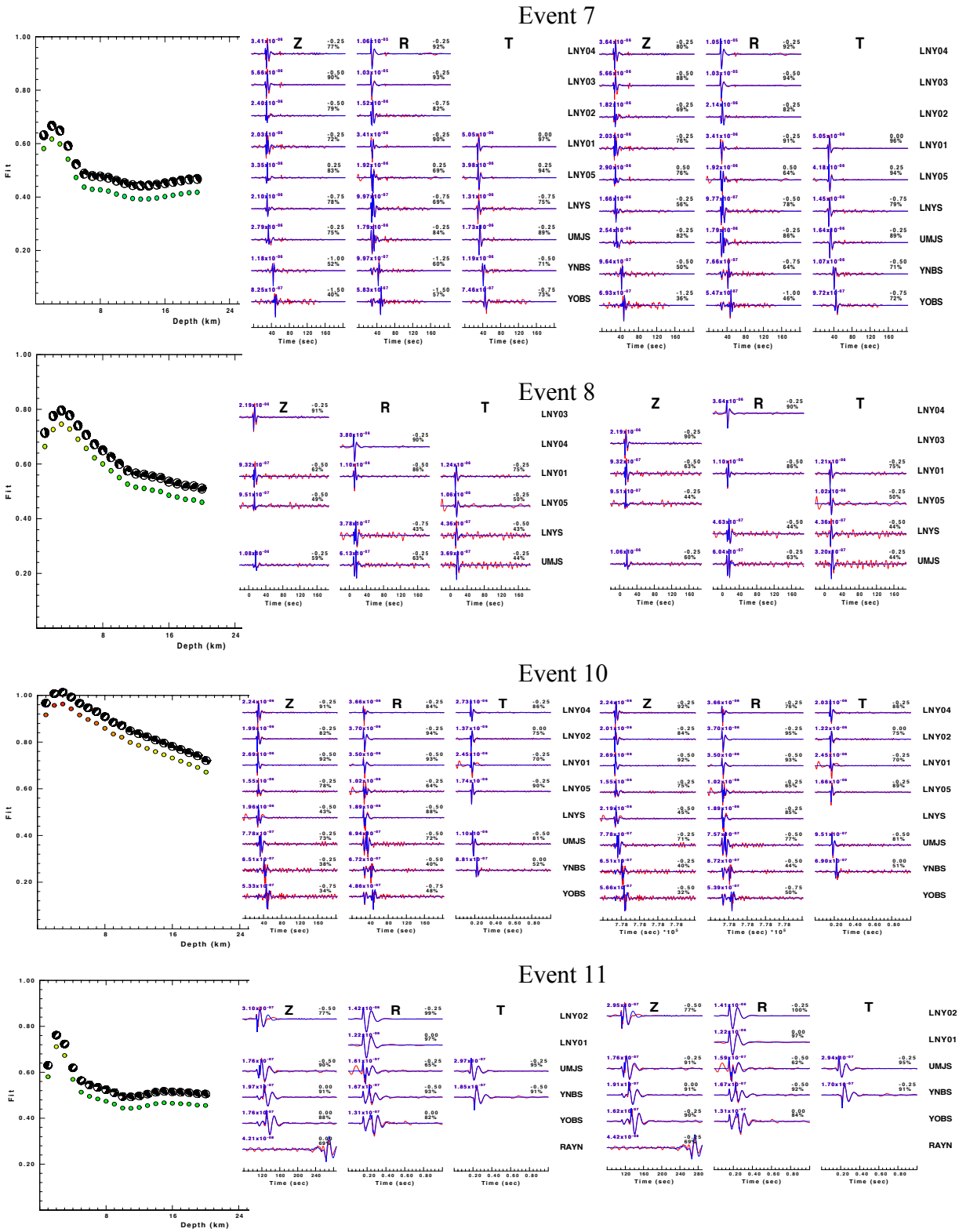

Figure 2 (continued).Results from the grid search and moment tensor inversion for source mechanisms for events in Saudi Arabia. The event numbers are the same as in Table 2. The panel on the left for each event shows the depth sensitivity of the goodness of fit parameter for the grid search. The panel of data in the middle shows the waveform fits for the grid search and the panel of data on the right is for the moment tensor inversion. The observed waveforms are in red and the matching synthetics are in blue for the best fitting solutions. The number on the top of the waveforms gives the time shift between the observed and synthetic waveforms. The focal mechanisms for the best fitting solutions are shown for each event in Figure 1.

Table 2 provides solutions for the eight events. The fault plane solutions obtained for the first 6 events listed shows aligned NW-SE tensional axes, which is consistent with previous findings (e.g. Pallister et al., 2010; Baer and Hamiel, 2010; Youssef, 2015), and is also in good agreement with tensional stress field associated with the Red Sea (Figure 1). Overall, the best fit was obtained for source depths ranging from 2 to 3 km, which is expected given the diking source for the main shock. The best double couple shows normal faulting with a NW-SE trend for the first 6 events in Table 2. The other two events exhibit NE-SW oriented mechanisms (Figure 1 and Table 2). The moment tensor elements and other source parameters obtained using Andrews' method (Andrews, 1986) are listed in Table 4 and 5, respectively.

Table 4. Moment tensor elements for GT5 events in Saudi Arabia.

Event #	xx ($\times 10^{22}$)	yy ($\times 10^{22}$)	xy ($\times 10^{22}$)	xz ($\times 10^{22}$)	yz ($\times 10^{22}$)	zz ($\times 10^{22}$)
1	0.0506	0.1481	0.0948	-0.0217	0.0281	-0.1988
3	8.4720	26.6100	17.8000	7.4170	14.9900	-35.0900
4	1.8500	3.7770	2.3310	0.2413	0.6244	-5.6280
5	178.9000	323.1000	232.1000	85.3100	112.0000	-502.0000
7	0.0880	0.3986	0.2330	0.0087	0.0293	-0.4866
8	0.0316	0.1216	0.0550	0.0033	0.0505	-0.1533
10	0.4035	0.4135	-0.3502	0.1697	-0.1300	-0.8170
11	0.1303	0.1423	-0.0874	0.0461	-0.0931	-0.2726

Event numbers are the same as in Table 2.

Table 5. Seismic source properties for Saudi Arabia events.

Event #	Moment $\times(10^{15})$ [N-M]	Corner Frequency [HZ]	Radiated Energy $\times(10^{8})$ [J]	Stress Drop [b] Brune	Stress Drop [b] Hanks
1	0.0014	5.2	9	37	43
3	0.2200 0.4200(CMT)	0.6	1000	14.5	40
4	0.0358	1.5	48	12.5	19.5
5	6.5400 3.9700(CMT)	0.3	2800	10	17
7	0.0058	2.5	6	10.5	19.5
8	0.0016	5	4	23.5	31
10	0.0055	2.1	1	11.5	17
11	0.0027	2.2	4	6.5	10

Source properties for GT5 events in Saudi Arabia for which source mechanisms were obtained. Event numbers are the same as in Tables 2 and 3. Red text shows GCMT results.

4.3. TANZANIA, EAST AFRICA GT RESULTS

Again, invoking the principal of criteria transfer, 32 earthquakes recorded on the 1994-1995 Tanzania Broadband Seismic Experiment network were identified based on the Kaapvaal craton criteria, and relocated. These events, located either on the Tanzania craton or just to the east of the craton in the Proterozoic Mozambique Belt, ranging in magnitude from 2.5 to 4.5, are shown on the map in Figure 3. Table 6 gives the event information for the 10 events with magnitudes equal to or greater than 3. Magnitudes shown are local magnitude determinations. The Tanzania Broadband Seismic Experiment consisted of 20 seismic stations recording continuously at 20 samples per second for 1 year. The GT events are clustered in the area where the two more-or-less linear arrays in the network (one W-E, one SW-NE) intersect, providing a dense enough station distribution to obtain GT5 event locations. The events were relocated using handpicked Pg arrival times in conjunction with a crustal velocity model from Langston et al. (2002). The data are publically available at IRIS.

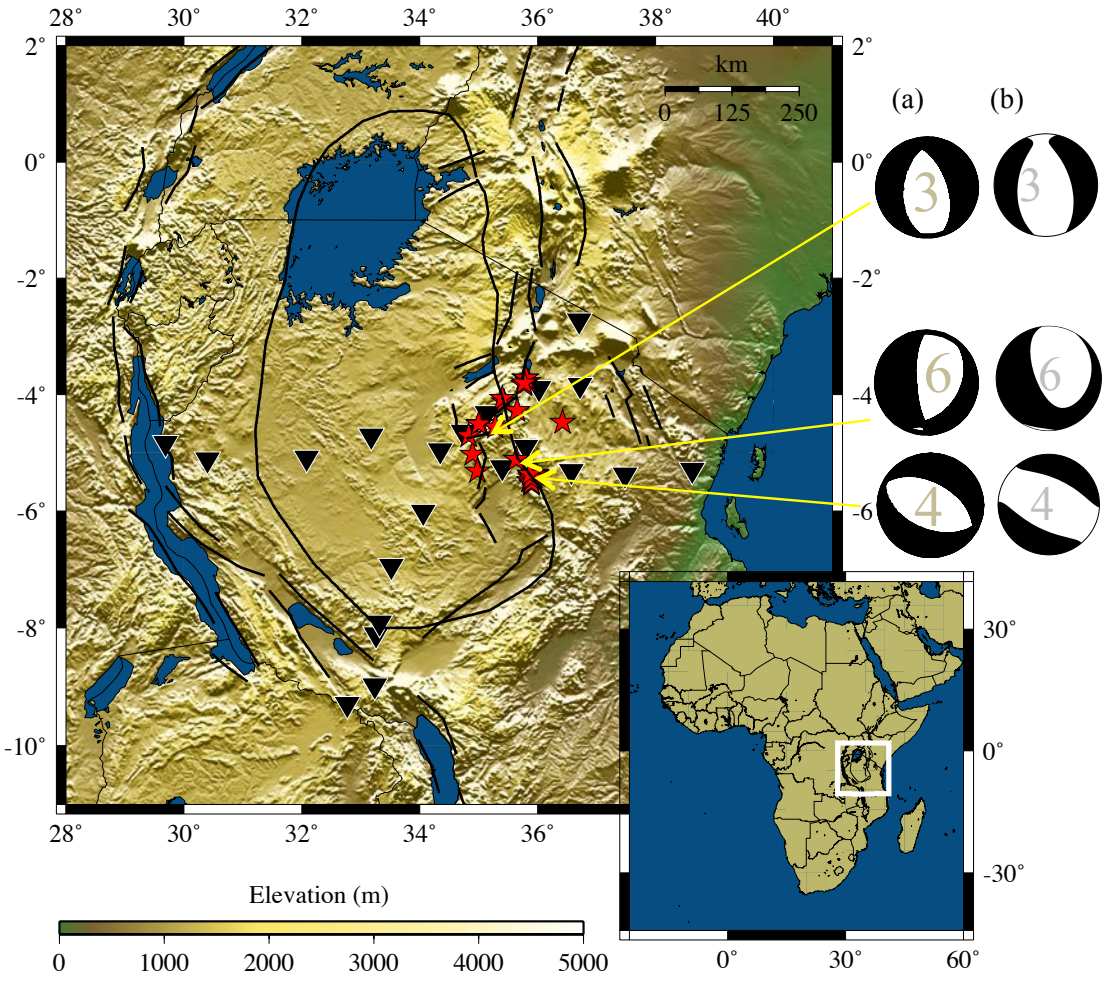

Figure 3. Map showing events, stations, and mechanisms for Tanzania. *Topographic map showing events (red stars) and seismic stations in Tanzania (inverted black triangles). Fault plane solutions are shown from the (a) grid search and (b) deviatoric moment tensor inversion for events listed in Table 7.*

4.4. TANZANIA, EAST AFRICA SOURCE PARAMETERS

Of the 10 earthquakes analyzed, we could obtain source parameters using the grid search and moment tensor inversion methods for only 3 of them (Table 7). The data for the other events were of insufficient quality to obtain stable modeling results. The velocity model used to calculate Green's functions is from Mulibo and Nyblade (2009) (Table 8). Figure 4 shows an example of the comparison between synthetic and observed waveforms for the events listed in Table 7 for their optimum depth. This figure also illustrates how the mechanism and goodness of the fit vary with depth for these events. Overall, the best fit was obtained for source depths ranging from 6 to 35 km. The fault plane solutions obtained illustrate normal faulting with NW-SE and NE-SW oriented nodal planes (Figure 3).

Table 6. Event locations and origin times for GT5 events in Tanzania with magnitudes of 3 or larger.

Event #	Year	Month	Day	Hour	Minute	Second	Latitude	Longitude	M_L
1	1994	7	20	11	32	2.82	-4.13	35.43	4.5
2	1994	7	13	0	42	35.71	-3.72	35.78	3.5
3	1994	10	2	11	1	54.63	-5.03	34.9	3.3
4	1994	8	27	2	4	5.46	-5.36	35.93	3.2
5	1994	8	17	3	23	34.32	-4.56	35.28	3.2
6	1994	10	21	2	30	46.91	-5.12	35.64	3.1
7	1994	9	28	14	10	48.9	-3.78	35.84	3
8	1994	9	22	4	34	53.74	-3.83	35.76	3
9	1994	7	24	9	58	2.73	-5.4	35.88	3
10	1994	8	4	15	42	17.05	-4.5	35.01	3

In Table 7, comparison of the goodness of the fit between the observed and calculated waveforms was performed using a grid search (DC), and Deviatoric Moment Tensor Inversion (DVMT). Percentages of CLVD and DC components estimated using these methods are listed in the last two columns. Depth, magnitude, strike, dip and rake from the deviatoric inversions are also listed. Event numbers are the same as in Table 6.

Table 7. Source parameters for Tanzanian events

Event #	Depth [km]	M_W	Goodness of the fit (%)		Strike	Dip	Rake	%CLVD, %DC
			DC	DVMT				
3	8	3.3	53	57	190/340	44/50	-68/-110	2,98
4	6	3.4	64	68	114/298	44/47	-93/-87	36,64
6	35	3.2	54	64	33/161	27/73	-41/-111	26,74

Table 8. 1D velocity model used to calculate Green's functions for events in Tanzania

Thickness (km)	*P*-wave velocity (km/s)	*S*-wave velocity (km/s)	Density (kg/m^3)
10	5.8400	3.3800	2330
10	6.2600	3.6300	2500
10	6.6800	3.8600	2670
7	7.0900	4.1000	2840
∞	8.2800	4.7400	3310

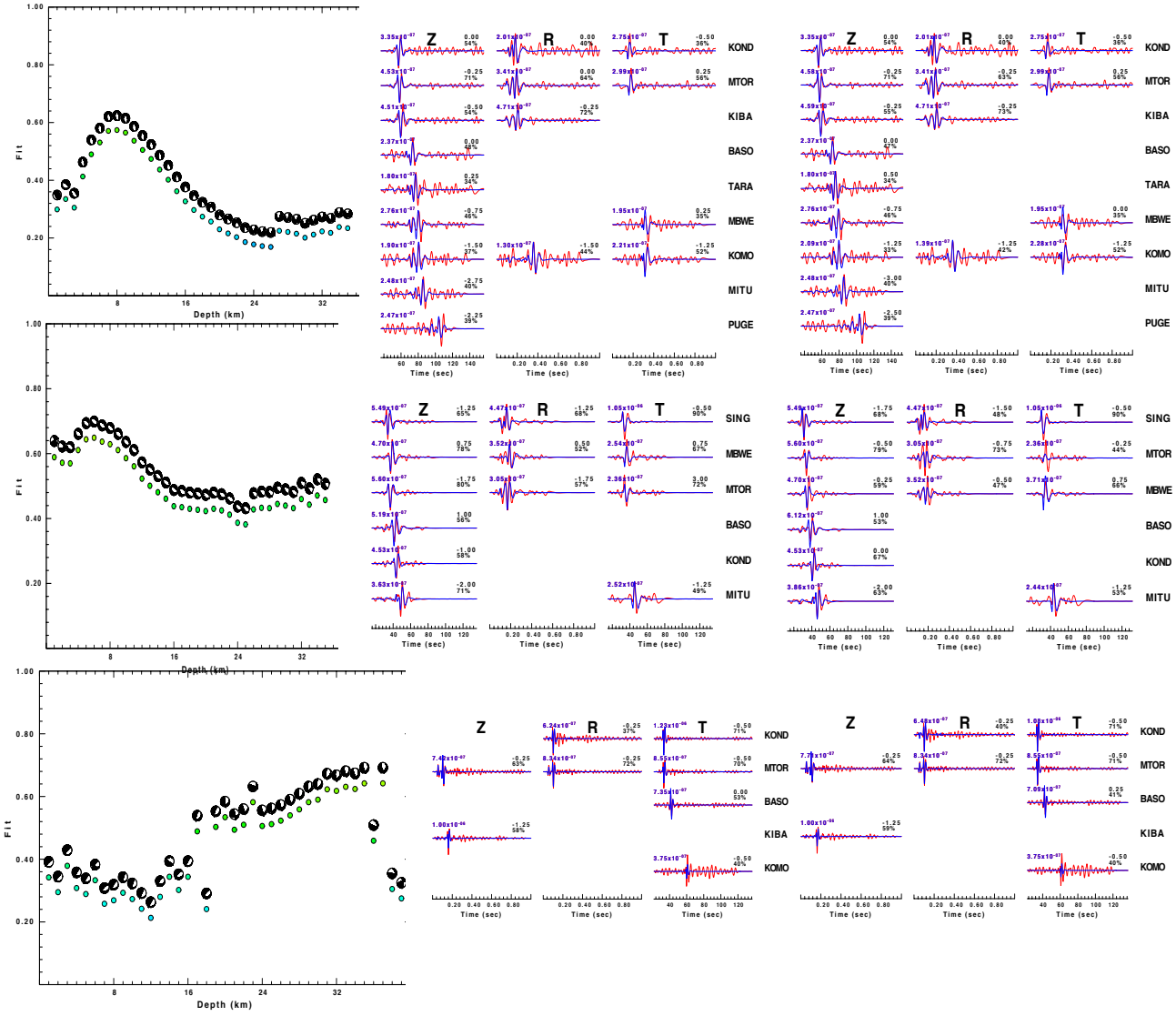

Figure 4. Results from the grid search and moment tensor inversion for source mechanisms for the three Tanzanian events in Table 7, in sequential order. *The panel on the left for each event shows the depth sensitivity of the goodness of fit parameter for the grid search. The panel of data in the middle shows the waveform fits for the grid search, and the panel of data on the right is for the moment tensor inversion. The observed waveforms are in red and the matching synthetics are in blue for the best fitting solutions. The number on the top of the waveforms gives the time shift between the observed and synthetic waveforms. The focal mechanisms for the best fitting solutions are shown for each event in Figure 3.*

The values of moment tensor elements and other source parameters such as radiated energy, stress drop, and seismic moments are listed in Tables 9 and 10.

Table 9. Moment tensor elements for GT5 events in Tanzania for which source mechanisms were obtained.

Event #	xx ($\times 10^{21}$)	yy ($\times 10^{21}$)	xy ($\times 10^{21}$)	xz ($\times 10^{21}$)	yz ($\times 10^{21}$)	zz ($\times 10^{21}$)
3	-0.0425	1.0720	0.1185	0.2554	0.1113	-1.0300
4	1.2150	0.0844	0.7452	0.0525	0.0676	-1.3000
6	-0.0486	0.5856	-0.1323	-0.3923	-0.6221	-0.5369

Event numbers are the same as in Table 6.

Table 10. Source properties for GT5 events in Tanzania for which source mechanisms were obtained.

Event #	Moment $\times(10^{17})$ [N-M]	Corner Frequency [HZ]	Radiated Energy $\times (10^{8})$ [J]	Stress Drop [b] Brune	Stress Drop [b] Hanks
3	0.0011	2.2	6	7.5	12.5
4	0.0014	1.9	4	5	8
6	0.0009	3.8	4	13	18.5

Event numbers are the same as in Table 6.

4.5. ETHIOPIA GT RESULTS

Boomer et al. (2013) reported 8 new GT5 for events for Ethiopia with magnitudes of 3 or greater (Table 11), obtained using earthquakes that occurred between 2001 and 2003 recorded by the Ethiopia Broadband Seismic Experiment (EBSE; Nyblade & Langston 2002) and the

Ethiopia Afar Geoscientific Lithospheric Experiment (EAGLE; Maguire et al. 2003; Bastow and Keir, 2011). Stations in these networks are located within the Main Ethiopian Rift and Afar Depression, and on the eastern and western sides of the Ethiopian Plateau (Figure 5).

Using criteria developed previously for the Main Ethiopian Rift (Boomer et al., 2013), we have extended the search for new GT events northward into the Afar Depression, identifying five new GT5 events with magnitudes greater than or equal to 4. These were recorded in 2007 and 2008 on a combination of stations from two temporary networks run by teams from the U.K. and three permanent regional stations of the AfricaArray network. The events were relocated using handpicked Pg arrival times in conjunction with a crustal velocity model from Boomer et al. (2013). The data are publically available at IRIS. Table 12 provides a list of these new GT5 events.

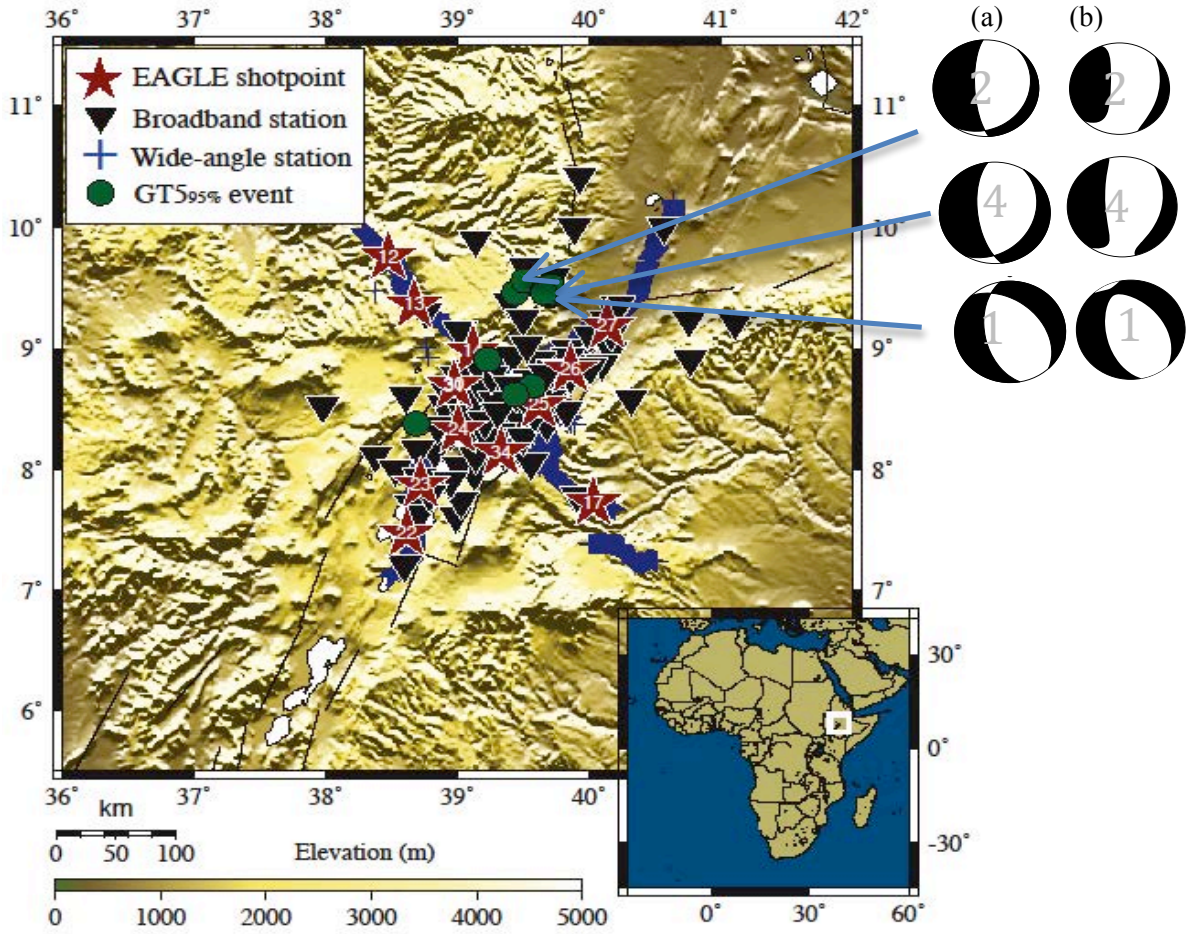

Figure 5. Map showing events, stations, and mechanisms for Ethiopia. *Topographic map showing GT events (green dots), broadband seismic stations locations (inverted black triangles), and short-period stations (cross). The stars show shots points. Fault plane solutions are shown from (a) the grid search and (b) deviatoric moment tensor inversion for events listed in Table 13.*

Table 11. GT5 events for Ethiopia from Boomer et al. (2013)

Event #	Year	Month	Day	Hour	Minute	Second	Latitude	Longitude	M_L
1	2001	5	23	01	16	10	9.460	39.44	3.6
2	2001	11	11	22	38	03	9.440	39.70	3.8
3	2001	12	13	02	14	40	9.460	39.69	3.1
4	2001	11	11	22	32	15	9.4563	39.6808	3.2
5	2001	12	13	02	14	38	9.4565	39.6963	3.2
6	2001	12	30	06	16	16	9.4682	39.6945	3
7	2002	2	17	02	38	16	9.4695	39.7025	3.2
8	2003	1	10	12	13	56	8.6125	39.4472	3.4

Table 12. New GT5 events for the Main Ethiopian Rift and Afar Depression.

Event #	Year	Month	Day	Hour	Minute	Second	Latitude	Longitude	M_L
1	2007	11	11	21	21	40	12.2323	40.7040	4.7
2	2008	10	17	09	40	40	12.3542	40.5938	4.9
3	2008	10	17	15	45	21	12.4085	40.5708	4.3
4	2008	10	17	20	24	24	12.3687	40.5942	4.5
5	2008	10	18	12	57	09	12.3702	40.6015	4

4.6. ETHIOPIA SOURCE PARAMETERS

The five GT events found in the Afar region (Table 12) were analyzed by Belachew et al. (2013) to obtain moment tensor solutions, and therefore we have not included them in our analyses for this project. Eight GT5 events within the main Ethiopian rift with magnitude equal to and greater than 3 identified by Boomer et al. (2013) listed in Table 11 have been analyzed. We were able to obtain source parameters using the grid search and moment tensor inversion methods for 3 of them (Tables 13 and 14). The data for the other events was of insufficient quality to obtain stable modeling results. The other source parameters obtained using Andrew's method (Andrews 1986) are listed in Table 15.

The velocity model used to calculate Green's function was adopted from Maguire et al., 2006 (Table 16). The region within and surrounding the Ethiopian Rift and Afar Depression is extremely heterogeneous and using a single velocity model did not result in good fits to the data.

To overcome this problem, four different velocity models associated with the western plateau, eastern plateau, northern part of the Main Ethiopian Rift, and the central part of the Main Ethiopian Rift, were used for stations located within these regions. Figure 6 shows the comparison between synthetic and observed waveforms for the events listed in Table 13 for their optimum depth. This figure also illustrates how the mechanism and goodness of the fit vary with depth for these events. The fault plane solutions achieved from both the grid search and moment tensor inversion demonstrate normal faulting with NW-SE and NE-SW orientation nodal planes.

In Table 13, comparison of the goodness of the fit between the observed and calculated waveforms was performed using a grid search (DC), and Deviatoric Moment Tensor Inversion (DVMT). Percentages of CLVD and DC components estimated using these methods are listed in the last two columns. Depth, magnitude, strike, dip and rake from the deviatoric inversions are also listed. Event numbers are the same as in Table 11.

Table 13. Source Parameters for Ethiopian Events

Event #	Depth [km]	M_W	Goodness of the fit (%)		Strike	Dip	Rake	%CLVD, %DC
			DC	DVMT				
1	10	3.5	69	74	170/316	52/43	-68/-116	0,100
2	7	3.8	62	64	37/177	22/73	-52/-104	46,54
4	7	3.3	50	51	31/174	31/64	-56/-109	19,81

Table 14. Moment tensor elements for GT5 events in Ethiopia for which source mechanisms were obtained.

Event #	xx ($\times 10^{21}$)	yy ($\times 10^{21}$)	xy ($\times 10^{21}$)	xz ($\times 10^{21}$)	yz ($\times 10^{21}$)	zz ($\times 10^{21}$)
1	0.3320	1.8620	1.0650	0.4634	-0.6363	-2.1940
2	-1.6050	4.3170	-1.3320	-0.1220	-4.8270	-2.7130
4	-0.1404	0.8319	-0.1993	-0.1601	-0.5686	-0.6914

Event numbers are the same as in Table 11.

Table 15. Source properties for GT5 events in Ethiopia for which source mechanisms were obtained.

Event #	Moment $\times(10^{17})$ [N-M]	Corner Frequency [HZ]	Radiated Energy $\times (10^{8})$ [J]	Stress Drop [b] Brune	Stress Drop [b] Hanks
1	0.012	0.7	7	1	7
2	0.015	1	38	3.5	4.5
4	0.004	1.4	6	2.5	2.5

Event numbers are the same as in Table 11.

Table 16. 1D velocity models used to caThe models in Table 16 from top to bottom are for the western plateau, eastern plateau, central part of the Main Ethiopian Rift, and northern part of the Main Ethiopian Rift.

Table 16. ID velocity models used to calculate Green's functions in Ethiopia

Thickness (km)	*P*-wave velocity (km/s)	*S*-wave velocity (km/s)	Density (kg/m^3)
4	5.0000	2.8571	2606
15	6.1300	3.5029	2743
10	6.3600	3.6343	2768
7	6.7300	3.8457	2807
14	7.3800	4.2171	2873
∞	8.0500	4.6000	2936

Thickness (km)	*P*-wave velocity (km/s)	*S*-wave velocity (km/s)	Density (kg/m^3)
1	4.4000	2.5143	2524
4	5.2000	2.9714	2632
9	6.1100	3.4914	2740
14	6.3400	3.6229	2766
13	6.7300	3.8457	2807
∞	8.0500	4.6000	2936

Thickness (km)	*P*-wave velocity (km/s)	*S*-wave velocity (km/s)	Density (kg/m^3)
1	3.0000	1.7143	2294
14	5.0000	2.8571	2606
17	6.0700	3.4686	2736
20	6.9000	3.9429	2825
∞	7.5000	4.2857	2884

Thickness (km)	*P*-wave velocity (km/s)	*S*-wave velocity (km/s)	Density (kg/m^3)
1	3.2000	1.8286	2331
3	5.1000	2.9143	2619
8	6.5000	3.7143	2783
1	6.6000	3.7714	2794
16	6.9000	3.9429	2825
∞	7.5000	4.2857	2884

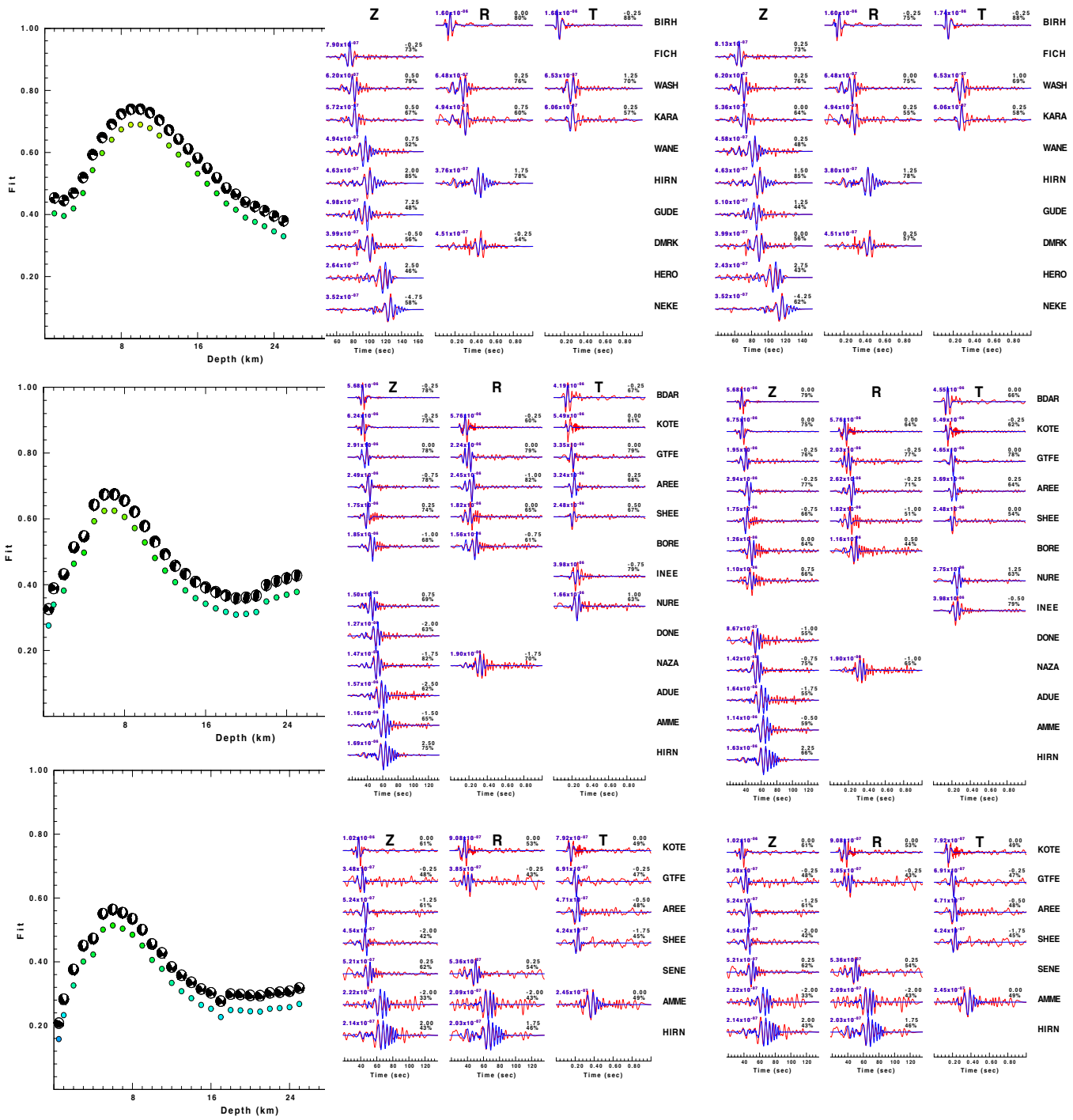

Figure 6. Results from the grid search and moment tensor inversion for source mechanisms for the three Ethiopian events in Table 13, in sequential order. *The panel on the left for each event shows the depth sensitivity of the goodness of fit parameter for the grid search. The panel of data in the middle shows the waveform fits for the grid search and the panel of data on the right is for the moment tensor inversion. The observed waveforms are in red and the matching synthetics are in blue for the best fitting solutions. The number on the top of the waveforms gives the time shift between the observed and synthetic waveforms. The focal mechanisms for the best fitting solutions are shown for each event in Figure 5.*

4.7. SOURCE PARAMETERS FOR EVENTS IN SAUDI ARABIA, TANZANIA, AND ETHIOPIA

As described previously, Andrews's method (1986) was used to calculate other seismic source parameters. This method was employed to find separate event and station spectra using the Spectral Value Decomposition (SVD) method. We calculated displacement, velocity, and acceleration power spectra for each event record. Each event's spectra was median-stacked and integrated up to the Nyquist frequency to determine displacement, velocity, and acceleration power spectra, which were then used to estimate corner frequency, radiated energy, seismic moment, and stress drop (equations 1-4). These parameters are illustrated in Figure 7. A high correlation between radiated energy and seismic moment (94% correlation) is observed, similar to previously reported studies (Beeler et al., 2003; Richardson & Jordan 2002).

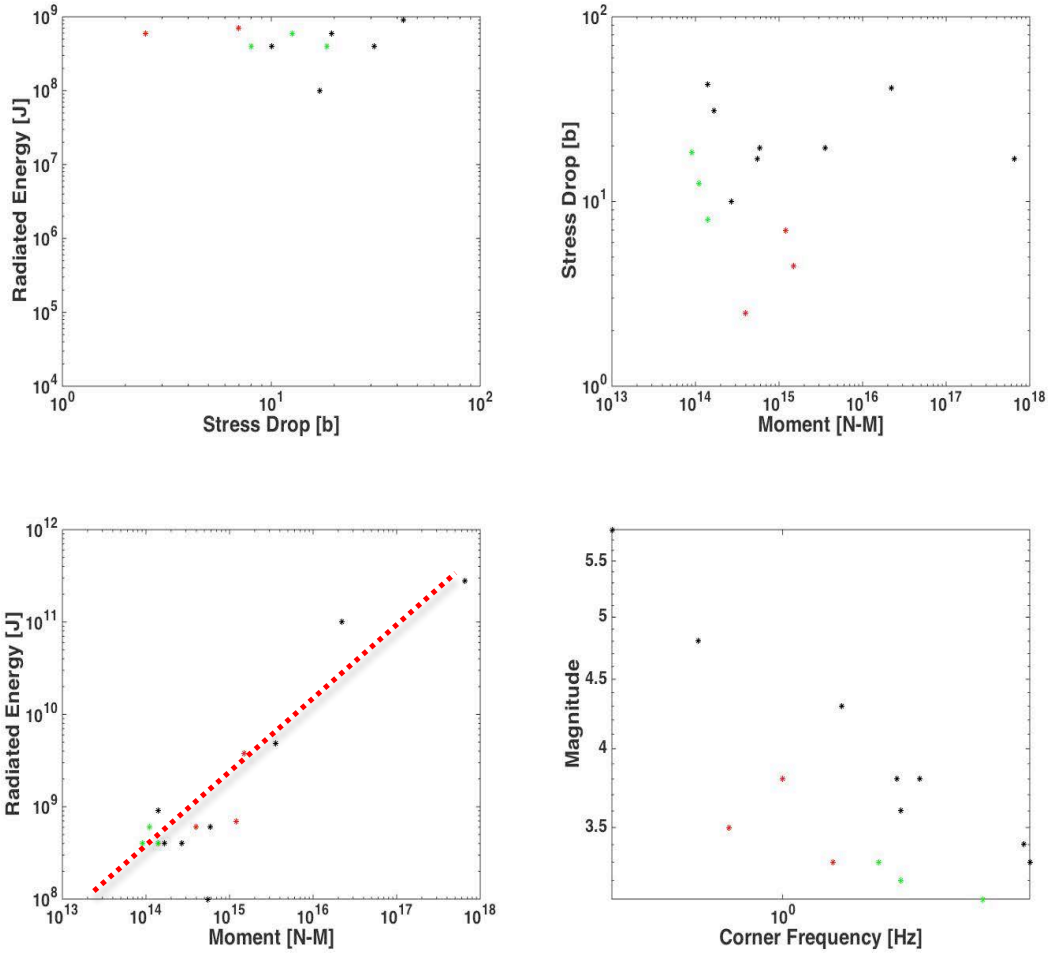

Figure 7. Plots of source parameters. *Plots of (top left) radiated energy versus stress drop, (top right) stress drop versus seismic moment, (bottom left) radiated energy versus seismic moment, and (bottom right) magnitude versus corner frequency. Black stars are data points for the events in Saudi Arabia, green stars are for the events in Tanzania, and the red stars are for the events in Ethiopia.*

5. SUMMARY AND CONCLUSIONS

In this project, Ground Truth (GT) 5 level seismic events in the Middle East and East Africa have been identified and a range of source properties for these events have been determined. The empirically based GT criteria developed by Boomer et al. (2010, 2013) has been used to identify 15 new GT5 events in Saudi Arabia, 5 in Ethiopia, and 10 in Tanzania with magnitudes of 3 or greater. Source parameters were obtained through moment tensor inversions for a number of the events where available waveforms were of sufficient quality. In addition, other source properties, such as seismic moment, stress drop, and corner frequency were also obtained for these events using the Andrews (1986) method. In total, given the quality of available data, we were able to obtained source parameters and other source properties for 8 events in Saudi Arabia, 3 in Tanzania, and 3 in Ethiopia.

REFERENCES

Andrews, D. J. (1986), Objective determination of seismic source parameters and similarity of earthquakes of different size, in Earthquake Source Mechanics, S. Das, J. Boatwright, C.H. Scholz, eds, vol. 6 of Geophysical Monograph 37, pp. 259-267, Am. Geophys. Union.

Baer, G. and G. Hamiel (2010), Form and growth of an embryonic continental rift: InSAR observations and modelling of the 2009 western Arabia rifting episode, Geophys. J. Int., Vol. 182, pp. 155-167.

Bastow, I.D. and D. Keir (2011), The protracted development of the continent-ocean transition in Afar, Nat. Geosci., Vol. 4, pp. 248-250, doi:10.1038/Ngeo1095.

Beeler, N. M., T. F. Wong, and S. H. Hickman, (2003), On the expected relationships among apparent stress, static stress drop, effective shear fracture energy, and efficiency, Bull. Seismol. Soc. Am., Vol. 93, pp.1381-1389.

Belachew, M., C. Ebinger, and D. Coté (2013), Source mechanisms of dike-induced earthquakes in the Dabbahu-Manda Hararo rift segment in Afar, Ethiopia: Implications for faulting above dikes, Geophys. J. Int., Vol. 192, pp. 907-917, doi: 10.1093/gji/ggs076.

Bondár, I, S. C. Myers, E. R. Engdahl, and E. A. Bergman (2004), Epicenter accuracy based on seismic network criteria, Geophys. J. Int, Vol. 156, pp. 483-496.

Bondár, I and K. L. McLaughlin (2009), A new ground truth data set for seismic studies, Geophys. Res. Lett., Vol. 80, pp. 465-472.

Boomer, K., R. Brazier, and A. Nyblade (2010), Empirically-based ground truth criteria for seismic events located using regional networks with application to southern Africa, Bull. Seism. Soc. Am., Vol. 100, pp. 8-21.

Boomer, K. B., R. A. Brazier, J. P. O'Donnell, A. A. Nyblade, J. Kokoska and S. Liu. (2013), From Craton to Rift: Empirically Based Ground-Truth Criteria for Local Events Recorded on Regional Networks, Bull. Seism. Soc. Am., Vol. 103 (4), pp. 2295-2304.

Carlson, R.W., T. L. Grove, M. J. de Wit, and J. J. Gurney (1996), Program to study the crust and mantle of the Archean craton in southern Africa. EOS, Trans. Am. Geophys. Union 77, pp. 273-277.

Hansen, S.E., H.R. DeShon, M.M. Driskell, and A.M.S. Al-Amri (2013), Investigating the Pwave Velocity Structure beneath Harrat Lunayyir, northwestern Saudi Arabia, using Double-Difference Tomography and Earthquakes from the 2009 Seismic Swarm, J. Geophys. Res., 118, pp. 1-13.

Herrmann, R. B. (2013), Computer programs in seismology: An evolving tool for instruction and research, Seism. Res. Lett., Vol. 84, pp. 1081-1088, doi:10.1785/0220110096.

Julia, J., C.J. Ammon, and R.B. Herrmann (2003), Lithospheric structure of the Arabian Shield from the joint inversion of receiver functions and surface wave group velocities, Tectonophysics, 371, pp. 1-21.

Kumar, M. R., D. Ramesh, J. Saul, D. Sarkar and R. Kind (2002), Crustal and upper mantle stratigraphy of the Arabian shield, Geophys. Res. Lett., Vol. 29 (10).

Langston, C. A., A. A. Nyblade, and T. J. Owens (2002), Regional wave propagation in Tanzania, East Africa, J. Geophys. Res., Vol. 107(B1), doi: 10.1029 /2001JB000167.

Madariaga, R. (1976), Dynamics of an expanding circular fault, Bull. Seis. Soc. Am., Vol. 66, pp. 639-666.

Maguire, P. K. H., C. J. Ebinger, G. W. Stuart, G. D. Mackenzie, K. A. Whaler, J. M. Kendall, M. A. Kahn, C. M. R. Fowler, S. L. Klemperer, G. R. Keller, S. Harder, T. Furman, K. Mickus, L. Asfaw, A. Ayele, and B. Abebe (2003), Geophysical Project in Ethiopia Studies Continental Breakup, Eos Trans. AGU 84, no. 5, pp. 342-343.

Maguire, P.K.H., G.R. Keller, S.L. Klemperer, G.D. Mackenzie, K. Keranen, S. Harder, B. O'Reilly, H. Thybo, L. Asfaw, M.A. Khan, and M. Amha (2006), Crustal structure of the northern Main Ethiopian Rift from the EAGLE controlled-source survey: a snapshot of incipient lithospheric break-up, in The Afar Volcanic Province within the East African Rift System, pp. 269-291, eds. G. Yirgu, C.J. Ebinger, and P.K.H. Maguire, Geological Society, London.

Mooney, W., M. Gettings, H. Blank, and J. Healy (1985), Saudi Arabian seismic-refraction profile: A travel time interpretation of crustal and upper mantle structure, Tectonophysics, Vol. 111, pp. 173-246.

Mulibo, G. and A. Nyblade (2009), The 1994–1995 Manyara and KwaMtoro earthquake swarms: variation in the depth extent of seismicity in northern Tanzania, S. Afr. J. Geol. Spec. AfricaArray Issue, Vol. 112 (3-4), pp. 387-404.

Nyblade, A. A. and C. A. Langston (2002), Broadband seismic experiments probe the East African rift, Eos Trans. AGU 83, 405, pp. 408-409.

Pallister, J.S., W.A McCausl, S. Jónsson, A.H.M. Lu, S. El Hadidy, A. Aburukbah, I.C.F. Stewart, P.R. Lundgren, R.A. White, and M.R.H. Moufti (2010), Broad accommodation of rift-related extension recorded by dyke intrusion in Saudi Arabia, Nature Geoscience, Vol. 3, pp. 705-712, doi: 10.1038/ngeo966.

Richardson, E. (2002), Earthquake nucleation and rupture at a range of scales: laboratories, gold mines, and subduction zones (Doctoral dissertation), Massachusetts Institute of Technology, Cambridge, MA.

Richardson, E., and T. H. Jordan (2002), Low-frequency properties of intermediate-focus earthquakes, Bull. Seism. Soc. Am., Vol. 92(6), pp. 2434-2448.

Youssef, S.E-H (2015), Seismicity and Seismotectonic Setting of the Red Sea and Adjacent Areas, in The Red Sea the Formation, Morphology, Oceanography and Environment of a Young Ocean Basin, pp. 151-159, eds. N. Rasul and I. Stewart, Springer Earth System Sciences.

APPENDIX

HYPOELLIPSE output for GT events and source depth from MT inversion.
Sminax = semi minor horizontal axis for 90% error ellipse in km
Smaxax= semi major horizontal axis for 90% error ellipse in km
Sdepth = vertical axis for 90% error ellipse in km

Saudi Arabia events:

Event #	Year	Month	Day	Hour	Minute	Second	Latitude	Longitude	Hypo. depth km	Sminax km	Smaxax km	Sdepth km	MT depth km
1	2009	5	18	23	43	36	25.292	37.7383	0	0.3	0.4	1.9	2
2	2009	5	19	15	50	45	25.2698	37.7542	0	0.3	0.4	2.8	-
3	2009	5	19	16	54	29	25.2712	37.7647	0.2	0.2	0.3	2.4	3
4	2009	5	19	17	13	26	25.291	37.7544	0	0.3	0.4	1.8	3
5	2009	5	19	17	34	59	25.2876	37.7483	0	0.3	0.4	2.9	2
6	2009	5	19	19	21	28	25.3001	37.755	0	0.3	0.3	2	-
7	2009	5	19	19	33	22	25.2948	37.7543	0	0.1	0.4	2.5	3
8	2009	5	19	19	44	19	25.3087	37.7591	5.7	0.3	0.4	0.7	3
9	2009	5	20	21	35	19	25.2447	37.7766	0	0.3	0.3	3	-
10	2009	5	21	22	3	16	25.2821	37.779	0	0.3	0.3	2.4	3
11	2009	5	30	8	31	58	25.2663	37.7801	3.4	0.2	0.2	0.3	2
12	2009	6	20	12	59	13	25.2709	37.7705	1.2	0.2	0.2	0.6	-
13	2009	6	22	11	2	43	25.2556	37.8014	10.9	0.4	0.6	0.5	-
14	2009	7	3	3	54	0	25.2487	37.791	6.6	0.2	0.3	0.2	-
15	2009	7	4	6	32	24	25.2517	37.7816	3.6	0.2	0.2	0.3	-

Tanzania events:

Event #	Year	Month	Day	Hour	Minute	Second	Latitude	Longitude	Hypo. depth km	Sminax km	Smaxax km	Sdepth km	MT depth km
1	1994	7	20	11	32	2.82	-4.13	35.43	72	0.2	0.4	0.8	-
2	1994	7	13	0	42	35.71	-3.72	35.78	28	0.3	0.5	0.5	-
3	1994	10	2	11	1	54.63	-5.03	34.9	11	0.2	0.3	0.5	8
4	1994	8	27	2	4	5.46	-5.36	35.93	8	0.2	0.4	0.6	6
5	1994	8	17	3	23	34.32	-4.56	35.28	21	0.2	0.3	0.5	-
6	1994	10	21	2	30	46.91	-5.12	35.64	43	0.2	0.4	0.9	35
7	1994	9	28	14	10	48.9	-3.78	35.84	15	0.3	0.3	0.6	-
8	1994	9	22	4	34	53.74	-3.83	35.76	4	0.2	0.5	0.8	-
9	1994	7	24	9	58	2.73	-5.4	35.88	13	0.3	0.4	0.6	-
10	1994	8	4	15	42	17.05	-4.5	35.01	14	0.2	0.4	0.5	-

Afar - Ethiopia events:

Event #	Year	Month	Day	Hour	Minute	Second	Latitude	Longitude	Hypo. depth km	Sminax km	Smaxax km	Sdepth km	*MT depth km
1	2007	11	11	21	21	40	12.2323	40.7040	0.4	0.2	0.4	0.9	1.5
2	2008	10	17	09	40	40	12.3542	40.5938	8.8	0.3	0.4	-	1.3
3	2008	10	17	15	45	21	12.4085	40.5708	0	0.2	0.2	0.9	0.9
4	2008	10	17	20	24	24	12.3687	40.5942	0	0.2	0.3	1.2	2.5
5	2008	10	18	12	57	09	12.3702	40.6015	0	0.3	0.4	2.2	8.2

* taken from Belachew et al. (2013)

Ethiopia events:

Event #	Year	Month	Day	Hour	Minute	Second	Latitude	Longitude	Hypo. depth km	Sminax km	Smaxax km	Sdepth km	MT depth km
1	2001	5	23	01	16	10	9.460	39.44	2				10
2	2001	11	11	22	38	03	9.440	39.70	0				7
3	2001	12	13	02	14	40	9.460	39.69	2				-
4	2001	11	11	22	32	15	9.4563	39.6808	14.3	1.2	18.1	5.5	7
5	2001	12	13	02	14	38	9.4565	39.6963	0	0.2	0.2	4	-
6	2001	12	30	06	16	16	9.4682	39.6945	7.4	0.2	0.3	0.7	-
7	2002	2	17	02	38	16	9.4695	39.7025	4				-
8	2003	1	10	12	13	56	8.6125	39.4472	12	0.2	0.2	0.5	-

DISTRIBUTION LIST

DTIC/OCP
8725 John J. Kingman Rd, Suite 0944
Ft Belvoir, VA 22060-6218 1 cy

AFRL/RVIL
Kirtland AFB, NM 87117-5776 2 cys

Official Record Copy
AFRL/RVBYE/Dr. Frederick Schult 1 cy

This page is intentionally left blank.